

Cobalt spin states and hyperfine interactions in LaCoO₃ investigated by LDA+*U* calculations

Han Hsu,¹ Peter Blaha,² Renata M. Wentzcovitch,¹ and C. Leighton¹

¹*Department of Chemical Engineering and Materials Science, University of Minnesota, Minneapolis, Minnesota 55455, USA*

²*Institute of Materials Chemistry, Vienna University of Technology, Getreidemarkt 9/165-TC, A-1060 Vienna, Austria*

(Received 23 August 2010; published 9 September 2010)

With a series of local-density approximation plus Hubbard *U* calculations, we have demonstrated that for lanthanum cobaltite (LaCoO₃), the electric field gradient at the cobalt nucleus can be used as a fingerprint to identify the spin state of the cobalt ion. Therefore, in principle, the spin state of the cobalt ion can be unambiguously determined from nuclear magnetic resonance spectra. Our calculations also suggest that a crossover from the low-spin to intermediate-spin state in the temperature range of 0–90 K is unlikely, based on the half-metallic band structure associated with isolated IS Co ions, which is incompatible with the measured conductivity.

DOI: [10.1103/PhysRevB.82.100406](https://doi.org/10.1103/PhysRevB.82.100406)

PACS number(s): 75.30.Wx, 71.15.Mb, 71.20.Ps, 76.60.Gv

The thermally induced spin-state crossover in lanthanum cobaltite (LaCoO₃) has been a source of much controversy for decades.^{1,2} At low temperature, LaCoO₃ is a diamagnetic insulator. All Co ions are in the low-spin (LS) state, with total spin $S=0$. As the temperature (T) is raised to ~ 90 K, it becomes paramagnetic with susceptibility $\chi(T) \propto T^{-1}$. As the temperature further increases to ~ 500 K, $\chi(T)$ shows a second anomaly, accompanied by an insulator-metal transition. At finite temperatures, Co ions could be in intermediate-spin (IS) or high-spin (HS) states, with $S=1$ or 2, respectively. The detailed mechanism of the spin-state crossover in the interval $0 < T < 90$ K remains highly controversial. It was first proposed to be an LS-HS crossover,³ but this was later questioned by a density-functional theory (DFT) calculation adopting the local-density approximation plus Hubbard *U* (LDA+*U*) method, in which an LS-IS crossover was implicated.⁴ Plenty of experimental results have subsequently been interpreted as supporting the LS-IS crossover,^{5–9} although evidence for the LS-HS crossover has also been presented.^{10–12} Such discrepancies also exist among theoretical works, including DFT calculations on bulks^{13–16} and atomic multiplet calculations on clusters.¹⁷

Clearly, some significant part of this confusion arises from the difficulty in reliably extracting the spin state from experimental data. For example, interpretations of x-ray emission spectroscopy (XES) (Ref. 7) or x-ray absorption spectroscopy (XAS) (Ref. 11) spectra rely on atomic multiplet calculations or the XES/XAS spectra of other well-known materials. Such XES ($K\beta'$) and XAS (L edge) spectra are difficult to compute with DFT for bulk materials. One well-known example is (Mg,Fe)SiO₃ perovskite, the most abundant mineral in the earth's lower mantle. The mechanism of its pressure-induced spin-state crossover is also highly debated. Similar XES ($K\beta'$) spectra have been interpreted in terms of both HS-LS (Ref. 18) and HS-IS (Ref. 19) crossovers. In the LaCoO₃ case, the XES ($K\beta'$) was interpreted as LS-IS (Ref. 7) while the XAS (Co $L_{2,3}$ edge) was interpreted as LS-HS.¹¹ Experiments with inelastic neutron scattering were also interpreted differently, even though their main results are similar.^{6,12}

Another way to probe the spin state of transition-metal ions, which has received relatively little attention, is through their nuclear hyperfine interaction (electric quadrupole interaction). The hyperfine interaction, a perturbation in general,

splits the degenerate energy level of a nucleus with spin I into sublevels with shifted energies $E_Q(m)$. To the first-order approximation,

$$E_Q(m) \approx eQV_{zz}/4I(2I-1) \times [3m^2 - I(I+1)], \quad (1)$$

where Q is the nuclear quadrupole moment, $V_{zz} \equiv \partial^2 V / \partial z^2|_{r=0}$ is the electric field gradient (EFG), V is the electric potential resulting from the surrounding electrons, and $m = -I, -I+1, \dots, I-1, I$.²⁰ The energy difference between these sublevels is called the quadrupole splitting (QS), which can be measured with techniques such as Mössbauer spectroscopy, or nuclear magnetic resonance (NMR) spectroscopy, via measurements of electric quadrupole frequency $\nu_Q \equiv 3eQ|V_{zz}|/2I(2I-1)h$. Since Q and I are intrinsic properties of the nucleus, any dependence of the QS on the spin state of the transition-metal ion comes from the dependence of the EFG on the orbital occupancy associated with each spin state. In general, Qs associated with different spin states are very distinguishable in Mössbauer spectroscopy, although the exact spin state cannot be determined solely based on the measured QS. By combining the EFG computed with DFT and the known Q and I , a theoretical QS can be obtained using Eq. (1). The spin state of the transition-metal ion can thus be identified by comparing the measured and computed QSs. This approach, as shown in Ref. 21, has successfully clarified the discrepancy among the interpretations of several Mössbauer spectroscopy measurements with essentially the same results in the (Mg,Fe)SiO₃ system.^{22–24}

A similar approach can be applied to LaCoO₃. In contrast to (Mg,Fe)SiO₃ perovskite where Fe-Fe interaction is negligible due to the low iron concentration ($\sim 10\%$), the interaction among Co ions in LaCoO₃ and its possible effect on the EFG should be investigated explicitly. We have done this by stabilizing magnetic Co ions (either IS or HS) under different conditions. These conditions correspond to different possible stages of the spin-state crossover, as shown in Fig. 1: (a) before crossover, all Co ions are LS; (b) early stage, single isolated magnetic Co ions are surrounded by LS ions; and late stage, all Co ions have the same $S (\neq 0)$, with ferromagnetic (FM) order (c), or G-type antiferromagnetic (AFM) order (d). To stabilize the states in Fig. 1, the inclusion of Hubbard *U* is necessary. We used LDA+*U* because it gives more accurate structural parameters.²⁵ We adopted the ex-

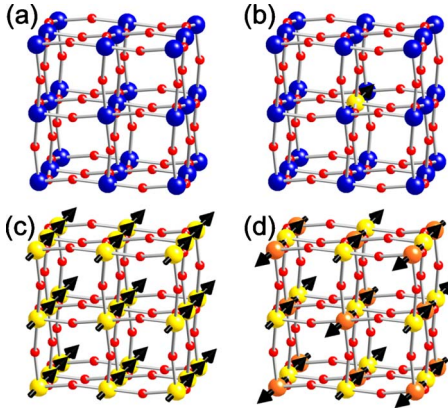


FIG. 1. (Color online) Possible stages of the thermally induced spin-state crossover, where larger spheres represent Co atoms, smaller spheres represent O atoms, and arrows show the spin moment. (a) Before crossover, all Co ions are LS; (b) early stage, low concentration (12.5%) of isolated magnetic Co ions; and late stage, all Co have the same $S (\neq 0)$, with (c) FM order or (d) G-type AFM order.

perimental lattice constants measured at $T=5$ K (Ref. 26) and relaxed the internal atomic structure. The structural relaxation was performed using the QUANTUM-ESPRESSO codes,²⁷ in which the pseudopotential method²⁸ is implemented. These states were also confirmed by all-electron calculations implemented in the WIEN2K code,²⁹ followed by EFG calculations. The early stage [Fig. 1(b)] was simulated by adopting supercells (with 40 or up to 320 atoms) containing one isolated magnetic Co. The remaining states in Fig. 1 can be treated with a ten-atom primitive cell. States with other magnetic ion concentrations or configurations can be stabilized as well, but that will not affect the Co nuclear EFG, as will be discussed later. We used a $3 \times 3 \times 3$, $6 \times 6 \times 6$, and $10 \times 10 \times 10$ \mathbf{k} -point mesh for the 320-, 40-, and 10-atom cells, respectively. The atomic relaxation is terminated when the interatomic forces are smaller than 2×10^{-4} Ry/bohr.

The EFGs of LS, IS, and HS Co in these different configurations are shown in Table I. We chose $U=5$ and 8 eV, our estimates for the lower and upper limit for Co, based on our calculation for LS Co,²⁵ and the decreasing Hubbard U with increasing spin moment.²¹ Remarkably, in each spin state and configuration, the EFG barely depends on the choice of Hubbard U . Because of the EFG's robustness with respect to the variation in U , calculating U from the first principles^{25,30-32} is not necessary for EFG calculations. Also, the EFG depends mainly on the spin state, irrespective of the concentration and configuration of magnetic ions. Therefore,

stabilizing states other than the ones in Fig. 1 is also unnecessary. The EFGs (in 10^{21} V/m²) of Co in different spin states are $V_{zz}^{(LS)} = -0.88 \pm 0.06$, $V_{zz}^{(IS)} = 12.8 \pm 1.1$, and $V_{zz}^{(HS)} = -20.3 \pm 2.0$. The corresponding QSs should thus be very distinguishable in NMR spectroscopy. With $Q = 0.42$ b (1 b $\equiv 10^{-28}$ m²) and $I = 7/2$ for the ⁵⁹Co nucleus, we have $\nu_Q^{(LS)} = 0.63 \pm 0.04$, $\nu_Q^{(IS)} = 9.3 \pm 0.8$, and $\nu_Q^{(HS)} = 14.7 \pm 1.8$ MHz. The computed $\nu_Q^{(LS)}$ is in good agreement with the experimental value 0.59 ± 0.01 MHz measured in the temperature range of 4.2–25 K,³³⁻³⁵ where LS Co dominates. This series of calculations indicates that, in principle, the spin state of Co ions can be unambiguously extracted from NMR spectra (the line broadening caused by shorter spin-spin and spin-lattice relaxation time with increasing temperature may be a potential problem), through all stages of the spin-state crossover.

The $3d$ orbitals of Co in LaCoO₃ are illustrated in Fig. 2, where the black thick segments represent Co-O bonds. These orbitals can be used to develop a physical understanding of the results shown in Table I. LaCoO₃ has a rhombohedrally distorted perovskite structure compressed along the $[111]$ direction (defined as the z axis). In such a crystal field (D_{3d} symmetry), the five $3d$ orbitals are grouped into two doublets and one singlet. One of the doublets has orbitals oriented toward oxygen, showing much e_g character [Fig. 2(a)], while the other has orbitals pointing away from oxygen [Fig. 2(b)]. The singlet, pointing away from oxygen, is exactly d_{z^2} [Fig. 2(c)]. For HS Co, the majority-spin electrons occupy all five orbitals, forming a spherically shaped charge distribution that gives a negligible EFG. $V_{zz}^{(HS)}$ is mainly contributed by the minority-spin electron, occupying the singlet d_{z^2} orbital that leads to a large (in magnitude) EFG.³⁶ For LS Co, the three orbitals pointing away from oxygen [Figs. 2(b) and 2(c)] are doubly occupied. The sum of these three orbitals [Fig. 2(d)] has a cubic-like shape, yielding a negligible EFG, so $V_{zz}^{(LS)} \approx 0$. For IS Co, a static Jahn-Teller distortion was not found in this work; all Co(IS)-O distances are the same. Three of its majority-spin electrons occupy the orbitals pointing away from oxygen, and the remaining one partially occupies the e_g -like doublet. Such an orbital occupancy barely contributes to $V_{zz}^{(IS)}$. The two minority-spin electrons occupy the doublet orbitals shown in Fig. 2(b). Their sum [Fig. 2(e)] leads to an EFG with a moderate magnitude. We therefore arrive at $|V_{zz}^{(LS)}| < |V_{zz}^{(IS)}| < |V_{zz}^{(HS)}|$, as shown in Table I.

When the Hubbard U is not calculated from the first principles, the computed total energy should not be used as a criterion to determine whether a LS-IS or LS-HS crossover is more likely for $0 < T < 90$ K. The electronic structures of the supercells containing isolated magnetic Co ions, however, can provide some hints. With 12.5% of isolated IS Co (40-

TABLE I. The EFG (in 10^{21} V/m²) of LS, IS, and HS Co in different atomic and magnetic configurations. EFG depends mainly on the spin state: $V_{zz}^{(LS)} = -0.88 \pm 0.06$; $V_{zz}^{(IS)} = 12.8 \pm 1.1$; $V_{zz}^{(HS)} = -20.3 \pm 2.0$.

| | LS | | IS | | HS | | |
|----------|----------|-------|-------|----------|--------|--------|--------|
| | Isolated | FM | AFM | Isolated | FM | AFM | |
| $U=5$ eV | -0.93 | 12.40 | 13.52 | 13.80 | -19.84 | -18.27 | -20.78 |
| $U=8$ eV | -0.82 | 11.69 | 13.17 | 13.88 | -21.86 | -22.29 | -21.78 |

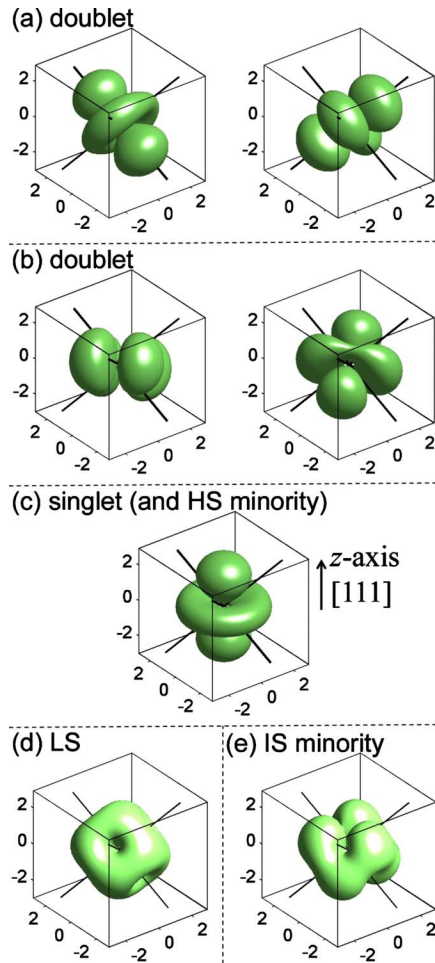


FIG. 2. (Color online) (a)–(c) The $3d$ orbitals of Co in the rhombohedrally distorted crystal field. The black thick segments represent Co-O bonds. The $[111]$ direction is aligned with the z axis. (d) Sum of the occupied orbitals in LS Co. (e) Sum of the orbitals occupied by the minority-spin electrons in IS Co. The minority-spin electron in HS Co occupies the orbital shown in (c).

atom supercell), LaCoO_3 is predicted to be half metallic, as demonstrated by the density of states (DOS), projected DOS (PDOS), and band structure shown in Fig. 3. Evident from the PDOS onto each Co site [Fig. 3(c)], the magnetic moment ($2 \mu_B/\text{cell}$) is mainly localized at the IS Co site. The first, second, and third neighbor shells of Co are essentially LS. The nonvanishing spin-up DOS at the Fermi level is contributed by the IS Co. The half-filled bands crossing the Fermi level [Fig. 3(d)] are formed by the above-mentioned partially occupied e_g -like doublet in IS Co. Even when the IS Co concentration is lowered to 1.56% (320-atom supercell), the half-metallic band structure persists, as shown in Fig. 4. As the IS Co concentration increases to 100%, LaCoO_3 remains conducting, with a half-metallic band structure when FM ordered, and a metallic one when AFM (G-type) ordered. It can thus be deduced that the LS-IS crossover is unlikely for $0 < T < 90$ K. Even with just a few percent of isolated IS Co, LaCoO_3 is predicted to be conducting, clearly incompatible with the conductivity measured in the same temperature range.³⁷ On the other hand, our calculations showed that LaCoO_3 is insulating with 12.5–50 % of isolated HS Co.

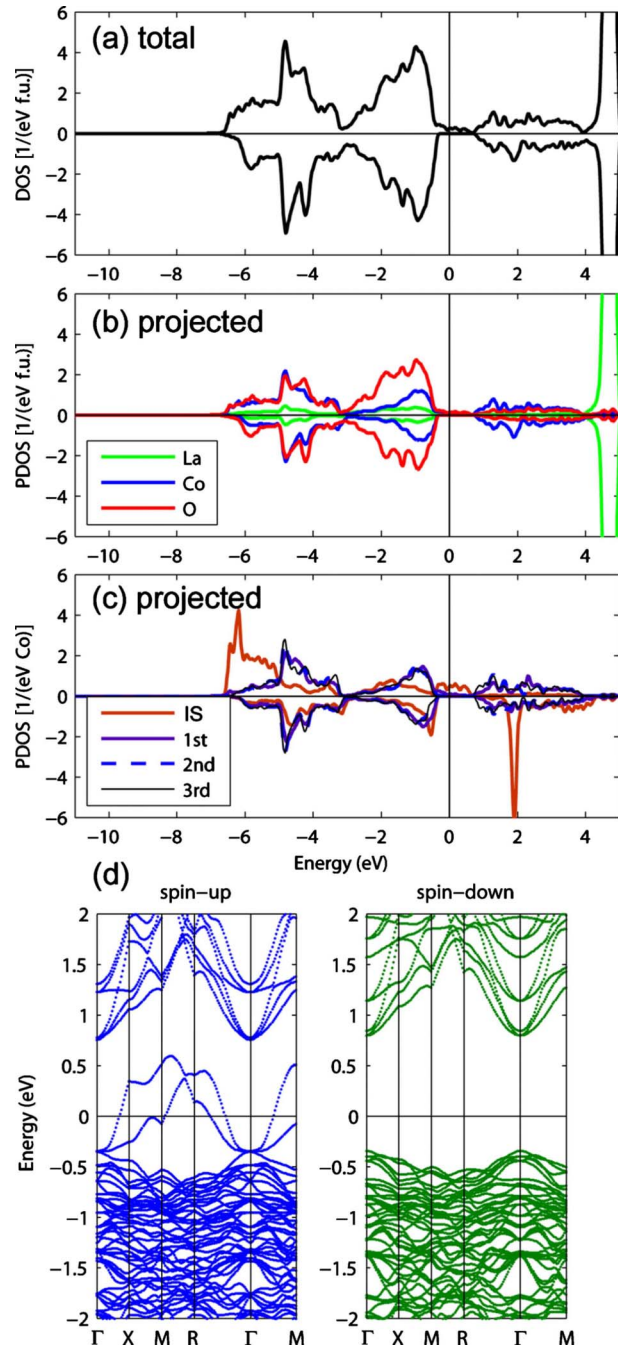


FIG. 3. (Color online) Electronic structure of the 40-atom supercell containing one IS Co. The Hubbard U is 5 eV for all spin states of Co. (a) Total density of states; (b) projected density of states on La, Co, and O; (c) projected density of states on the IS and surrounding LS Co; and (d) band structure.

With 100% of HS Co, LaCoO_3 is insulating when AFM ordered (G-type). When FM ordered, $U=5$ eV produces a metallic state while $U=8$ eV produces an insulating state. However, the HS-AFM state is more energetically favorable than the HS-FM state for any given U , consistent with the negative Weiss temperature extracted from $\chi(T)$ in the 100–500 K region. Thus, excitation of HS Co in the interval 0–90 K should not result in conducting LaCoO_3 , consistent with experiments.

In summary, we have stabilized LaCoO_3 in various states

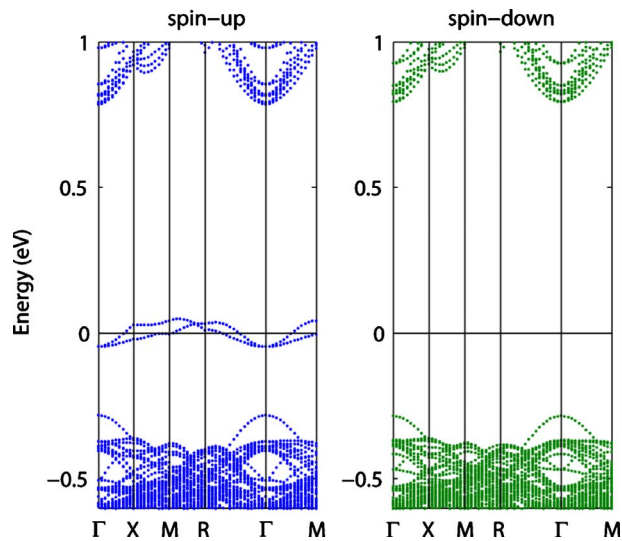


FIG. 4. (Color online) Band structure of the 320-atom supercell containing one IS Co. The Hubbard U is 5 eV for all spin states of Co.

that correspond to possible stages of the low-temperature spin-state crossover. In each case, the electronic structure and the electric field gradient at the Co nucleus were computed. The EFG depends primarily on the spin state of Co, irrespective of the choice of Hubbard U , the concentration of magnetic Co ions, and the specific form of magnetic order. Therefore, the EFG can be used as a fingerprint to identify the spin state of Co. This indicates that, in principle, the spin state of Co can be unambiguously extracted from NMR spectra. We have also demonstrated that the LS-IS crossover from 0–90 K is unlikely, due to its metallic band structure incompatible with the measured conductivity.

This work was primarily supported by the MRSEC Program of NSF under Awards No. DMR-0212302 and No. DMR-0819885, and partially supported by Grants No. EAR-0810212 and No. ATM-0426757 (VLab). P.B. was supported by the Austrian Science Fund (P20271-N17). C.L. acknowledges additional support from DOE under Grant No. DE-FG02-06ER46275 and NSF under Grant No. DMR-0804432. The authors thank Michael Hoch for the discussion on NMR spectroscopy. Calculations were performed at the Minnesota Supercomputing Institute (MSI).

- ¹J. B. Goodenough, *Localized to Itinerant Electronic Transition in Perovskite Oxides* (Springer, New York, 2001), and references therein.
- ²C. N. R. Rao *et al.*, *Top. Curr. Chem.* **234**, 1 (2004), and references therein.
- ³P. M. Raccach and J. B. Goodenough, *Phys. Rev.* **155**, 932 (1967).
- ⁴M. A. Korotin *et al.*, *Phys. Rev. B* **54**, 5309 (1996).
- ⁵S. Yamaguchi, Y. Okimoto, and Y. Tokura, *Phys. Rev. B* **55**, R8666 (1997).
- ⁶D. Phelan *et al.*, *Phys. Rev. Lett.* **96**, 027201 (2006).
- ⁷G. Vankó, J.-P. Rueff, A. Mattila, Z. Németh, and A. Shukla, *Phys. Rev. B* **73**, 024424 (2006).
- ⁸R. F. Klie *et al.*, *Phys. Rev. Lett.* **99**, 047203 (2007).
- ⁹T. Takami, J. S. Zhou, J. B. Goodenough, and H. Ikuta, *Phys. Rev. B* **76**, 144116 (2007).
- ¹⁰S. Noguchi, S. Kawamata, K. Okuda, H. Nojiri, and M. Motokawa, *Phys. Rev. B* **66**, 094404 (2002).
- ¹¹M. W. Haverkort *et al.*, *Phys. Rev. Lett.* **97**, 176405 (2006).
- ¹²A. Podlesnyak *et al.*, *Phys. Rev. Lett.* **97**, 247208 (2006).
- ¹³I. A. Nekrasov, S. V. Streltsov, M. A. Korotin, and V. I. Anisimov, *Phys. Rev. B* **68**, 235113 (2003).
- ¹⁴K. Knížek, P. Novák, and Z. Jirák, *Phys. Rev. B* **71**, 054420 (2005).
- ¹⁵K. Knížek *et al.*, *J. Phys.: Condens. Matter* **18**, 3285 (2006).
- ¹⁶K. Knížek, Z. Jirák, J. Hejtmánek, P. Novák, and W. Ku, *Phys. Rev. B* **79**, 014430 (2009).
- ¹⁷Z. Ropka and R. J. Radwanski, *Phys. Rev. B* **67**, 172401 (2003), and references therein.
- ¹⁸J. Badro *et al.*, *Science* **305**, 383 (2004).
- ¹⁹J. Li *et al.*, *Proc. Natl. Acad. Sci. U.S.A.* **101**, 14027 (2004).
- ²⁰H. M. Petrilli, P. E. Blochl, P. Blaha, and K. Schwarz, *Phys. Rev. B* **57**, 14690 (1998), and references therein.
- ²¹H. Hsu *et al.*, *Earth Planet. Sci. Lett.* **294**, 19 (2010).
- ²²J. M. Jackson *et al.*, *Am. Mineral.* **90**, 199 (2005).
- ²³J. Li *et al.*, *Phys. Chem. Miner.* **33**, 575 (2006).
- ²⁴C. McCammon *et al.*, *Nature Geosci.* **1**, 684 (2008).
- ²⁵H. Hsu, K. Umemoto, M. Cococcioni, and R. Wentzcovitch, *Phys. Rev. B* **79**, 125124 (2009).
- ²⁶P. G. Radaelli and S.-W. Cheong, *Phys. Rev. B* **66**, 094408 (2002).
- ²⁷P. Giannozzi *et al.*, *J. Phys.: Condens. Matter* **21**, 395502 (2009).
- ²⁸D. Vanderbilt, *Phys. Rev. B* **41**, 7892 (1990). We used valence electronic configurations $5s^2 5p^6 5d^1 6s^1 6p^1 4f^0$, $3s^2 3p^6 3d^6 4s^2 4p^0$, and $2s^2 2p^4$ for La, Co, and O, respectively. Core radii are $r_s=r_p=r_d=2.2$ a.u. and $r_f=1.7$ a.u. for La, $r_s=r_p=r_d=1.8$ a.u. for Co, and $r_s=r_p=1.4$ a.u. for O. The energy cutoffs are 48 and 192 Ry for wave function and charge density, respectively.
- ²⁹P. Blaha *et al.*, in *WIEN2k, An Augmented Plane Wave Plus Local Orbitals Program for Calculating Crystal Properties*, edited by K. Schwarz (Technische Universität Wien, Vienna, 2001).
- ³⁰M. Cococcioni and S. de Gironcoli, *Phys. Rev. B* **71**, 035105 (2005).
- ³¹H. J. Kulik, M. Cococcioni, D. A. Scherlis, and N. Marzari, *Phys. Rev. Lett.* **97**, 103001 (2006).
- ³²V. Leiria Campo, Jr. and M. Cococcioni, *J. Phys.: Condens. Matter* **22**, 055602 (2010).
- ³³M. Bose, A. Ghoshray, A. Basu, and C. N. R. Rao, *Phys. Rev. B* **26**, 4871 (1982).
- ³⁴M. Itoh *et al.*, *J. Phys. Soc. Jpn.* **64**, 970 (1995).
- ³⁵Y. Kobayashi, N. Fujiwara, S. Murata, K. Asai, and H. Yasuoka, *Phys. Rev. B* **62**, 410 (2000).
- ³⁶P. Dufek, P. Blaha, and K. Schwarz, *Phys. Rev. Lett.* **75**, 3545 (1995).
- ³⁷S. R. English, J. Wu, and C. Leighton, *Phys. Rev. B* **65**, 220407(R) (2002).